Content list available at ICONSMAT

Journal of Construction Materials

Journal homepage: www.iconsmat.com.au/publication

Article history:
Received 27 September 2020
Received in revised form
17 October 2020
Accepted 27 October 2020
Available online
2 January 2021

Prediction of the module of elasticity of green concretes containing ground granulated blast furnace slag using hybridized multi-objective ANN and Salp swarm algorithm

Amirreza Kandiri[1]*, Fahimeh Fotouhi[2]

[1] Institute of Construction Materials, Tehran, Iran

[2] Department of computer engineering, Bu-Ali Sina University

*Corresponding author: E: amir.kandiri@iconsmat.com.au

Abstract

Ground granulated blast furnave slag (GGBFS) once used in concrete derives both technical and economic advantages. Energy consumption and greenhouse gas emissions can be reduced significantly if cement is replaced by GGBFS in concrete mixtures. However, it is necessary to develop a detailed model in order to evaluate the elastic modulus of the concretes containing GGBFS because of important role of its value as a parameter in different design codes. In addition, it can save energy, cost, and time in comparison to direct laboratory-based measurements. In this research, to develop a model for the estimation of the elastic modulus of concretes containing GGBFS, Artificial neural network (ANN) was used. A multi-objective optimization method titled multi-objective slap swarm algorithm (MOSSA) was proposed to optimize the error and complexity of the developed ANN models. To develop predictive models of elastic modulus. Besides, one of the most used classification techniques to solve engineering problems that is The M5P model tree algorithm was used in order to develop predictive models of elastic modulus. The efficiency of the proposed model developed based on the ANN algorithm was compared with that of the model developed based on the M5P model tree technique with the help of several error measures. The result of this research is that it is possible using the M5P model tree and the proposed ANN model for the purpose of provide predictive tools for estimating the elastic modulus of concretes containing GGBFS and these would have 13.36% and 1.79% mean absolute percentage error (MAPE), respectively. It is understood from these values that the proposed model based on ANN algorithm is much more effective than the one developed using M5P model tree.

DOI: 10.36756/JCM.v2.2.2

Keywords

Concrete module of elasticity; Ground granulated blast furnace slag; Artificial neural network; Multi-objective optimization; Salp swarm algorithm, M5P model tree

Introduction

Concrete is the most popular material in construction that is using to build bridges, ports, buildings to name a few. The most important ingredients of concrete are cement (C), water (W), coarse aggregate (CA), and fin aggregate (FA). However, around a ton of carbon dioxide is emitted during the producing a ton of cement. In fact, cement production has a major contribution in global greenhouse gas emission [1–5].

One of the best solution for this problem is replacing cement with supplementary cementitious materials (SCMs) such as fly ash, silica fume, and ground granulated blast furnace slag, to name a few. This solution has been being used significantly in the past two decades. Using SCMs not only does reduce the greenhouse gas emission, but also improves mechanical properties and durability of concrete [6].

GGBFS is by product of manufacturing pig iron containing calcium oxide (30-50%), silicon dioxide (28-38%), aluminum oxide (8-24%), and magnesium oxide (1-18%), and it is made by cooling the molten slag rapidly. This process make GGBFS fine, granular, and almost glassy with unstable hydraulic properties [7–9]. GGBFS and other SCMs affect concrete hardening phase and its strength development. Therefore, the predictive models, which were developed to estimate elastic modulus of ordinary concrete, are not so useful for type of concrete. Hence, there is a need for developing a especial model to estimate elastic modulus of concrete containing GGBFS.

Recently artificial intelligence tools (AI) especially artificial neural networks (ANN) have been used to predict mechanical properties and behavior of different concretes. Moreover, metaheuristic algorithms have been used to reduce ANNs' errors. The models, which have been developed recently, have a better performance than old one like genetic algorithm or particle swarm optimization algorithm. For instance, in a study multi-objective salp swarm algorithm hybridized with ANN to predict compressive strength of concrete with GGBFS [10]. In another study multi-objective grey wolf optimization algorithm and an ANN used to predict compressive strength of concrete containing silica fume [11]. Table. 1 represents recent works that used ANNs to predict mechanical properties of concrete such as compressive strength (CS), elastic modulus (EM), flexural strength (FS), split tensile (ST), and creep coefficient (CC).

Due to the effect of ANN's architecture on its performance, it is necessary to obtain the ANN with the optimum architecture. On the other hand, having an accurate model comes with unwanted cost of time. Therefore, in this research a multi-objective optimization algorithm named multi-objective salp swarm algorithm (MOSSA) is used to optimize accuracy and complexity of the ANN. This approach makes it possible to obtain a network with essential complexity and accuracy. Furthermore, the results of the proposed model will be compare with a popular model named M5P tree to test its performance.

Table 1 A list of previous research on the applications of various AI-based techniques in concrete industry.

Concrete type	Property	AI model
Concretes containing GGBFS	CS	ANN, M5P[10]
Concrete containing waste foundry sand	CS, FS, EM, ST	M5P[12]
Normal and high-strength concretes with fly ash and/or GGBFS	CS	M5P [13], Fuzzy logic [14], ANN [6,14–17]
High-performance concrete made with copper slag and nanosilica	CS	Regression analysis and ANN [18]
Concretes containing fly ash and/or GGBFS	CS	ANN [14]
Concretes containing construction and demolition waste	CS	ANN [19]
Concretes containing fly ash and silica fume	CS	ANN [20]
Self-compacting concrete (SCC)	CS	ANN [21,22]
Silica fume concrete	CS	ANN [23], Fuzzy logic [23], hybrid ANN with multi-objective grey wolves [11], biogeography-based programming (BBP) [24]
Lightweight concrete	CS	ANN [25,26]
Environmentally friendly concrete	CS	Hybrid ultrasonic-neural prediction [27], ANN [28],
Concrete containing agricultural and construction wastes	CS	ANN [29]
Normal and high-performance recycled aggregate concrete	CS, EM, FS, ST	multiple nonlinear regression and ANN [30]
Recycled aggregate concrete	EM	M5P [31], genetic programming, artificial bee colony programming, and BBP [32], ANN, fuzzy TSK, and radial basis function neural network, and support vector regression [33]
Steel fiber-reinforced concrete	ST	ANN, SVR, and M5P [34]
SCC	EM	BBP and ABCP [35]
Concretes containing waste foundry sand	CS, EM, FS, ST	M5P [36]

Data collection

In this research, a comprehensive database consist of 131 different experimental records of concretes that made with GGBFS was collected from the literature in order to develop the models for the prediction of the elastic modulus [37–43]. In all mixes, the curing conditions were not changed. The only parameter which was used as output in this study is the cylinder (150 millimeters by 300 millimeters) elastic modulus (EM) of concrete. For experimental records with other types of samples, for the purpose of obtaining the target elastic modulus values, conversion factors were used[44]. Six potentially impressive factors were considered as input variables. In fact, they were in three main categories that are the amounts of constituents in the concrete mix and the testing age (TA) of concrete. Concrete compositions included amounts of cement, GGBFS, water (W), fine aggregate (FA) and coarse aggregate (CA). Fig.1 represented the input and the output variables' histograms. Moreover, statistical values of input and output variables are given in Table 2.

Table 2 Statistical values of input and output variables.

Statistical values	C (Kg/m^3)	W (Kg/m^3)	GGBFS (Kg/m^3)	CA (Kg/m^3)	FA (Kg/m^3)	TA (Days)	EM (MPa)
Minimum	33.0	109.0	0.0	1040.0	482.0	3.0	8.3
Maximum	541.0	203.0	315.0	1242.0	839.0	180.0	50.3
Mean	254.2	169.5	121.4	1130.8	674.0	56.6	25.1
Standard deviation	107.3	23.1	92.0	39.6	61.2	56.9	10.7
Skewness	0.3	-1.5	0.1	0.5	-1.4	1.1	0.6
Kurtosis	-0.3	1.3	-1.1	1.8	4.4	-0.1	-0.4

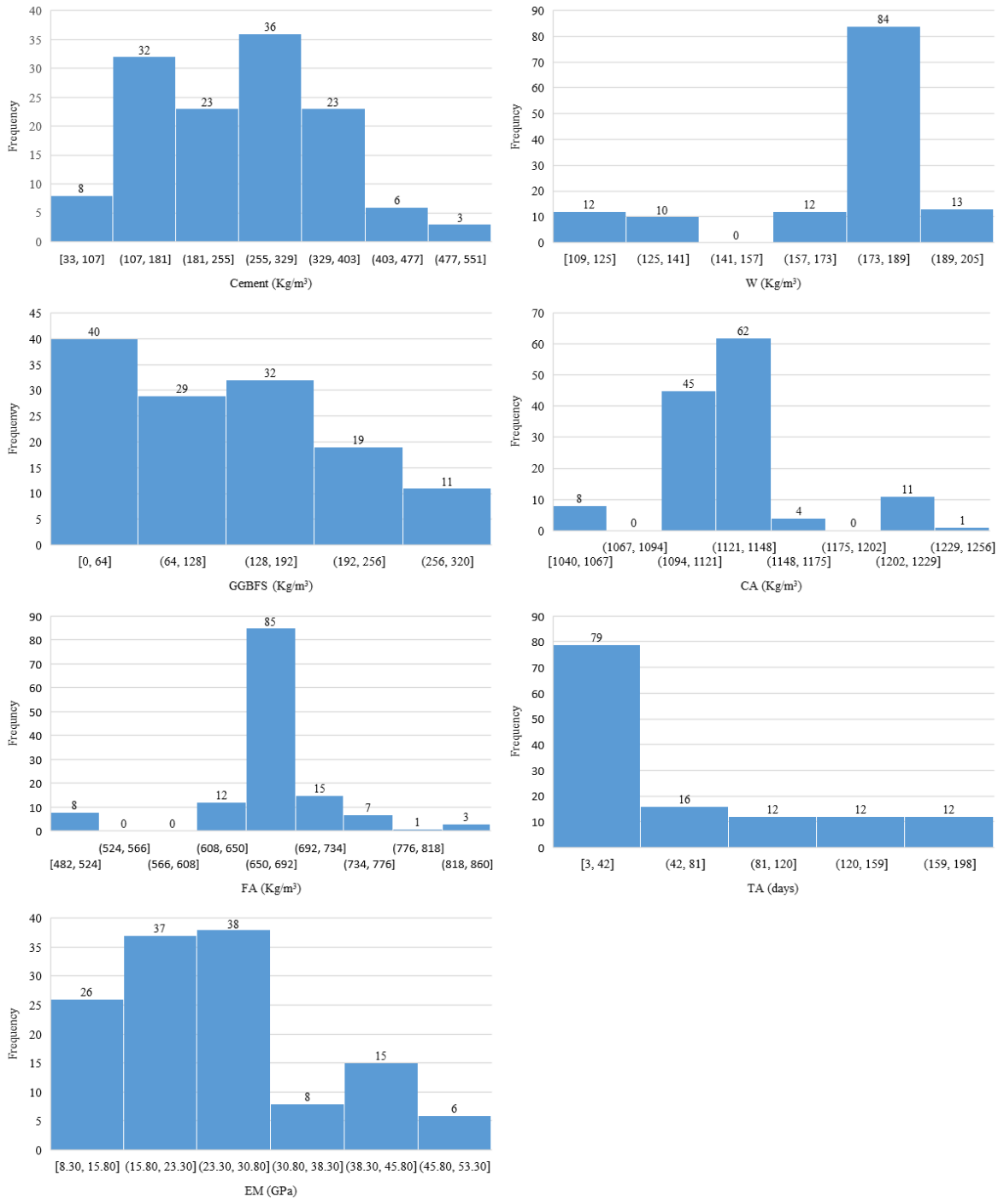

Figure 1 The histograms of input and the output variables.

Methodology

To determine the architecture of an ANN, the most used method is trial-and-error. There will be a change in speed and accuracy of an ANN if number of hidden layers and their neurons is changed. Therefore, for generating ANN models that have different complexities and accuracies, developing a model with this ability is seriously needed. In this study, to develop a multi-objective artificial neural network (MOANN) [10], salp swarm algorithm that is a multi-objective optimization algorithm is combined with an ANN[45]. In Fig. 2 different stages of proposed MOANN are illustrated. Then the

outputs of an M5P tree [46,47] and MOANN were compared to test performance of the proposed model.

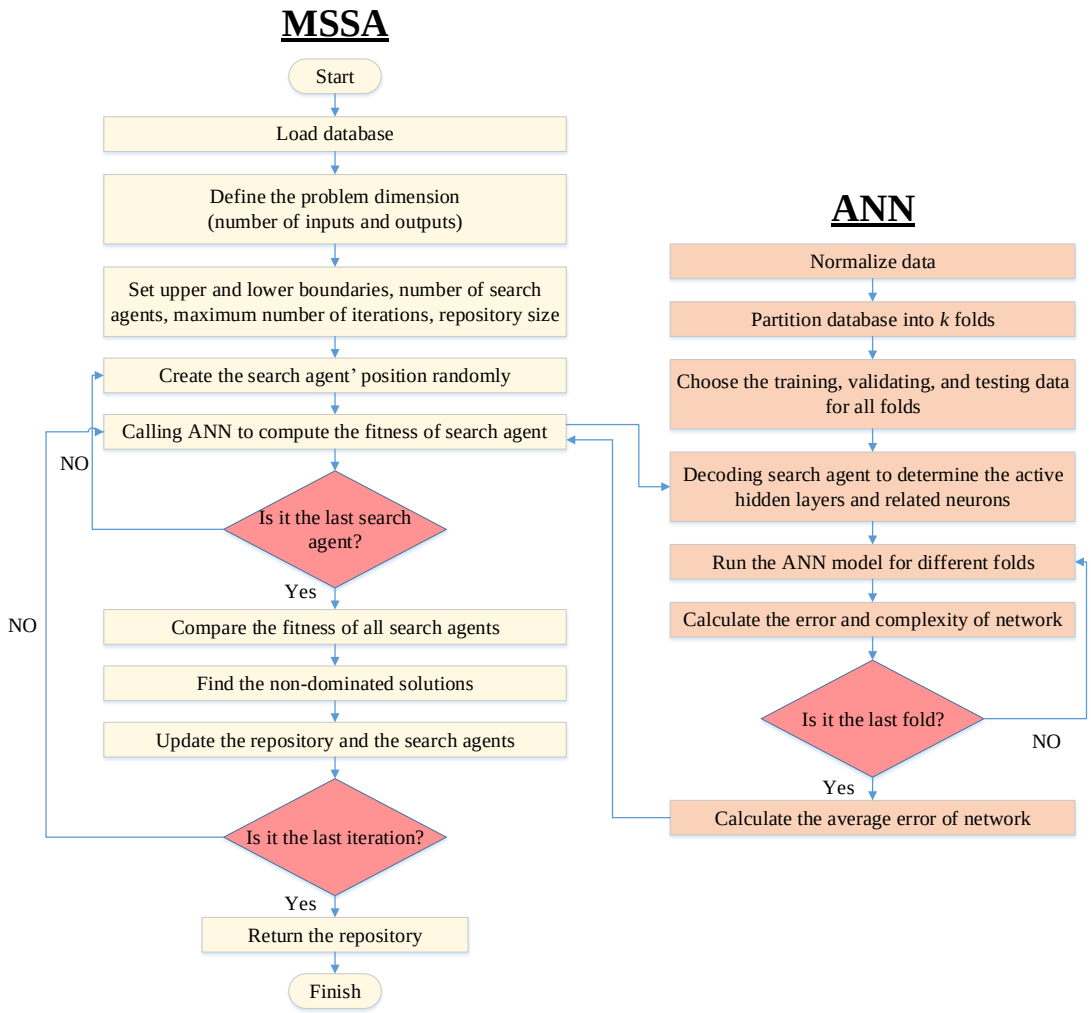

Figure 2 Different stages of the proposed MOANN

Results and discussion

Adjustment parameters of the proposed model should be determined before its running and they consist of the maximum number of hidden layers, the maximum number of neurons in each hidden layer, the activation function type in hidden and output layers, the ANN training method, the total runs number, the number of maximum iteration, the number of salps, and the size of the repository. With the help of the trial-and-error technique, all these adjustment parameters were achieved and they are represented in Table 3.

Table 3 Adjustment parameters of the proposed model.

Parameters	Values
Maximum number of hidden layers	3
Maximum number of neurons in each hidden layer	16
Hidden layers' activation function	Hyperbolic tangent sigmoid
Output layer's activation function	Linear
ANN training algorithm	Levenberg-Marquardt
Number of total runs	10
Maximum iteration number	100
Salp number	30
Repository size	50

After 10 times of running the model, the best Pareto front was discovered which is consist of OBJ and complexity that are two objective functions and showed in Fig. 3 in the vertical and horizontal axes, respectively. 150,000 ANN models that did not have the same architecture were developed to reach the Pareto front, and in the long run, the optimal ANN models were represented by 12 non-dominated salps. As can be seen in Fig. 3 with decreasing the value of OBJ, the complexity enhances and it can be understood that the more accurate prediction of the elastic modulus of concrete containing GGBFS is possible with more complicated architecture ANN models.

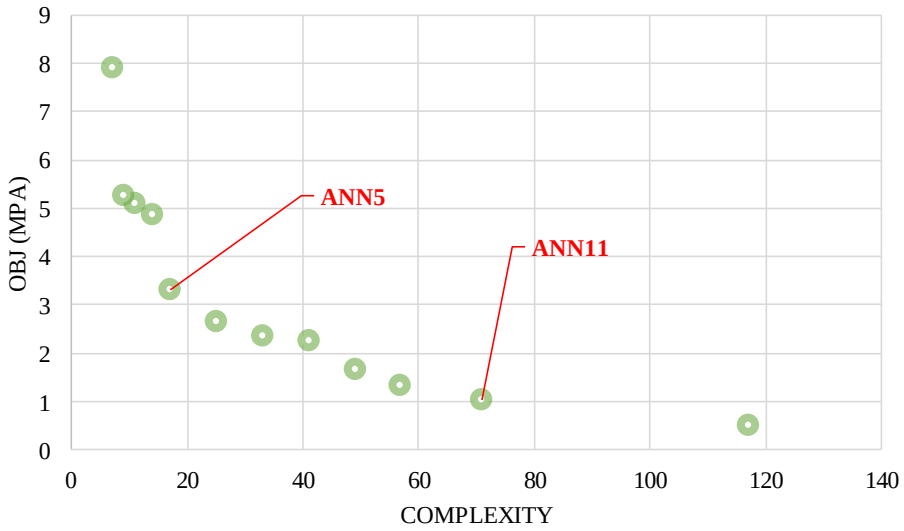

Figure 3 Pareto front of the proposed model.

More statistical indicators other than those mentioned in the previous section were used for the purpose of comparing the performances of the developed models with different architectures. These statistical indicators were scatter index (SI), mean bias error (MBE), and mean absolute percentage error (MAPE), which are formulated as follows:

$$\mathrm{SI} = \mathrm{RMSE}/\overline{\mathrm{E}} \tag{13}$$

$$\mathrm{MBE} = \frac{1}{\mathrm{P}}\sum_{\mathrm{i=1}}^{\mathrm{P}}(\mathrm{M_p} - \mathrm{E_p}) \tag{14}$$

$$\mathrm{MAPE} = \frac{100}{\mathrm{P}}\sum_{\mathrm{i=1}}^{\mathrm{P}}\frac{\mathrm{M_P}-\mathrm{E_P}}{\mathrm{M_P}} \tag{15}$$

All parameters are as defined previously, but $\overline{\mathrm{E}}$ is the average value of the experimental results. If SI < 0.1, an ANN model has an "excellent performance", if 0.1 < SI <0.2, a "good performance", if 0.2 < SI < 0.3, a "fair performance", or if SI > 0.3, a "poor performance"[48]. The architectures, statistical indicators, and complexities of the optimal ANN models for all data are given in Table 4.

Table 4 Non-dominated salps information for all data.

ANN	Architecture	OBJ (MPa)	RMSE (MPa)	MAPE (%)	MAE (MPa)	R	SI	MBE (MPa)	Complexity
ANN-1	6-1	7.90	5.20	20.71	3.90	0.77	0.21	0.31	7
ANN-2	6-1-1	5.25	3.62	14.76	2.81	0.88	0.14	0.35	9
ANN-3	6-1-1-1	5.10	3.61	14.62	2.76	0.89	0.14	0.05	11
ANN-4	6-1-2-1	4.85	3.52	14.64	2.72	0.89	0.14	0.31	14
ANN-5	***6-2-1***	***3.33***	***2.72***	***8.33***	***1.69***	***0.94***	***0.11***	***0.12***	***17***
ANN-6	6-3-1	2.65	2.34	7.32	1.41	0.95	0.09	0.03	25
ANN-7	6-4-1	2.35	2.06	6.53	1.20	0.96	0.08	-0.10	33
ANN-8	6-5-1	2.25	1.88	6.70	1.28	0.97	0.07	-0.04	41
ANN-9	6-6-1	1.66	1.15	3.80	0.79	0.99	0.05	0.00	49
ANN-10	6-7-1	1.34	0.73	2.34	0.50	1.00	0.03	-0.01	57
ANN-11	***6-5-5-1***	***1.05***	***0.77***	***1.79***	***0.39***	***0.99***	***0.03***	***-0.02***	***71***
ANN-12	6-8-6-1	0.52	0.28	0.83	0.17	1.00	0.01	0.00	117

The fact that how much the forecasted values are matched to the experimental ones is represented by the Pearson correlation coefficient (R). In addition, it demonstrates how much R values of 8 networks out of 12 optimal networks are more than 0.90.

ANN-12 with OBJ value of 0.52 MPa, RMSE of 0.28 MPa, MAPE of 0.83 percent, MAE of 0.17 MPa, R-value of 1, SI value of 0.01, MBE of 0.00 MPa, and complexity of 117, which makes it the most complex one with 6-8-6-1 architecture, is the most accurate network. Unlike ANN-12, ANN1 is the simplest since it has complexity value of seven, OBJ value of 7.90 MPa, RMSE of 5.20 MPa, MAPE of 20.71, MAE of 3.9 MPa, R-value of 0.77, SI value of 0.21, and MBE of 0.31 MPa, which causes it to be the least accurate one that has no hidden layer. For different structure the MBE values calculated and they indicate that elastic modulus of concrete containing GGBFS are overestimated by eight networks while it is underestimated by four ANN models. It can be understood from the SI that performance of seven networks are excellent, four networks are good, just one is fair, and none of them is poor. The two ANN models that are shown in Fig.3 were selected for more research since unlike their complexity rise significantly, they have minimal reduction in the next networks' error. Fig. 4 illustrated these two networks (i.e., ANN-5 model that has two neurons in its only hidden layer and ANN-11 model with 6-5-

5-1 architecture). The OBJ value of the ANN-11 model in comparison with the ANN-5 model, is about 68% less, but it has a higher R-value by 5 points. However, ANN-11 model has 71 links, which is more than four times the ANN-5 links. The ANN-11, ANN-5, and ANN-1 models' OBJ values are higher than the ANN-12 model; In fact, they are higher by 101%, 540%, and 1419%, respectively. Moreover, the ANN-1 model's RMSE is 91% more than ANN-5 model, while the value of this parameter in the ANN-11 is higher than that of the ANN-12 model by almost 175%. On the other hand, according to SI indicator, the ANN-12 and ANN-11 models have excellent performance while the ANN-5 has good performance and ANN-1 has fair performance, respectively. The fact that in contrast to the ANN-11 model, the ANN-1 and ANN-5 models overestimate, can be understood from MBE. Additionally, the value of MBE in the ANN-19 that is zero causes an accurate estimation for this model. The weights and biases of the ANN-11 and ANN-5 models are given in the appendix.

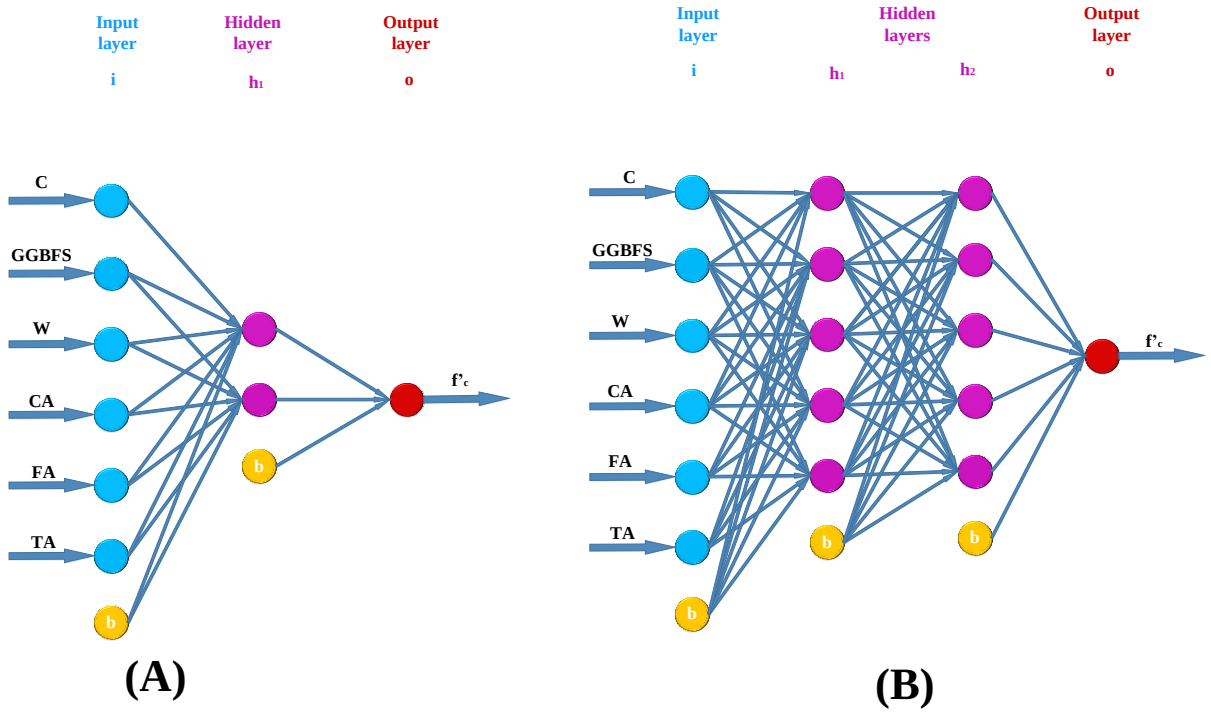

Figure 4 Architectures of (A) ANN-5 and (B) ANN-11.

In order to have a better comparison, comparing the results of ANN-16 and ANN-7 with the results of M5P model tree was done. Table 5 shows the coefficients that are predicted for the M5P model tree and Fig. 5 illustrates the obtained tree model.

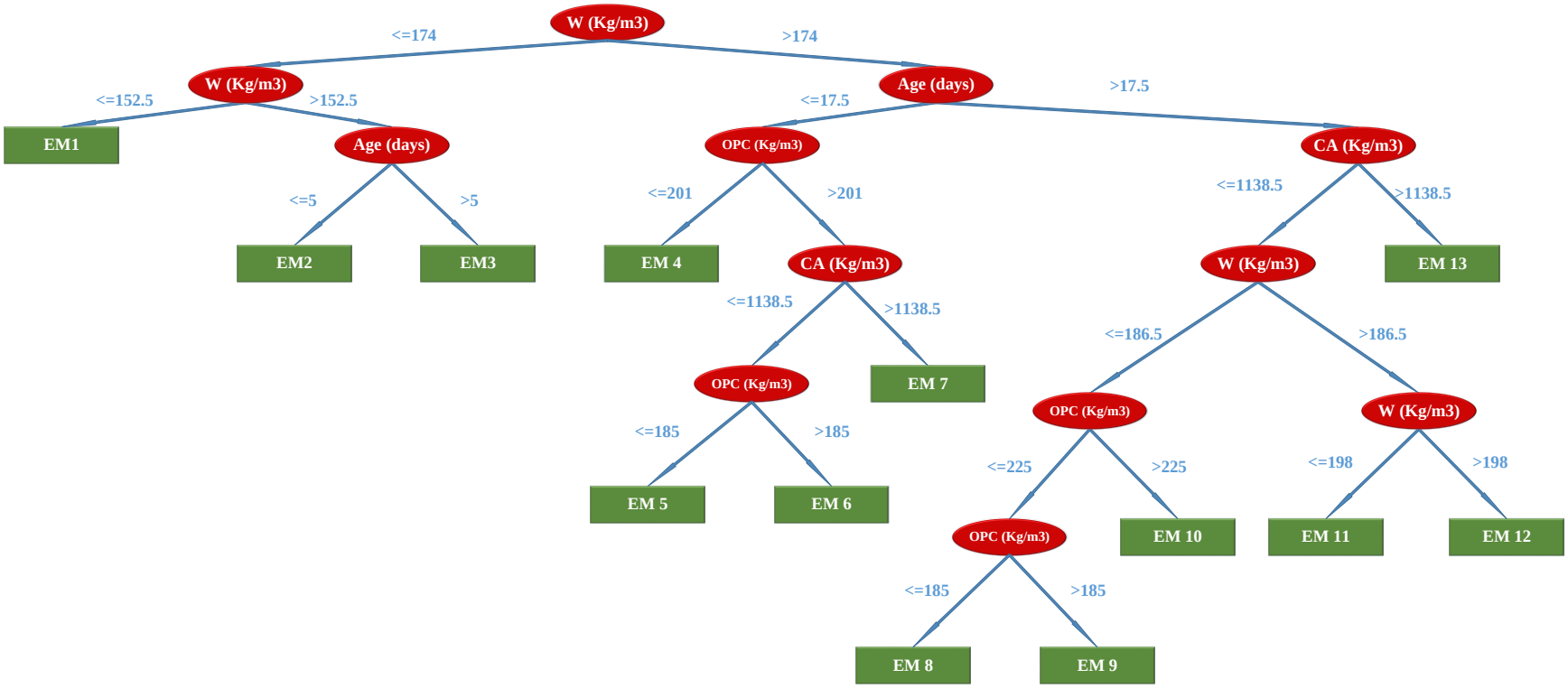

Figure 5 Regression M5P model tree for EM of concrete containing GGBFS.

Table 5 Predicted coefficients for the M5P model tree.

Linear models	Coefficients						
	OPC	W	GGBFS	CA	FA	TA	Bias
EM 1	0.0228	-0.0961	0.0266	0.0166	-0.0222	0.1029	40.1120
EM 2	0.0358	-0.1591	0.0266	0.0166	-0.0003	0.0186	22.3479
EM 3	0.0358	-0.1591	0.0266	0.0166	-0.0003	0.1773	22.8905
EM 4	0.0190	-0.0413	0.0039	-0.0260	0.0060	0.4458	40.7597
EM 5	0.0037	-0.0413	0.0016	-0.0174	0.0060	0.4552	36.0793
EM 6	0.0137	-0.0413	0.0016	-0.0174	0.0060	0.4842	33.4584
EM 7	0.0125	-0.0413	0.0016	-0.0174	0.0060	0.4676	33.5757
EM 8	0.0317	0.0001	0.0094	0.0073	0.0060	0.0159	0.7881
EM 9	0.0224	0.0001	0.0094	0.0073	0.0060	0.0085	2.7532
EM 10	0.0263	0.0919	0.0094	0.0073	0.0060	0.0188	-14.6676
EM 11	0.0214	-0.5182	0.0094	0.0073	0.0060	0.0109	102.3652
EM 12	0.0234	-0.4726	0.0094	0.0073	0.0060	0.0109	91.3902
EM 13	0.02	-0.1094	0.0094	0.0073	0.0060	0.0207	18.9997

The statistical indicators of ANN-11, ANN-5, and M5P tree models are given in Table 6. It is observed that the value of RMSE indicator of the ANN-5 is 253% more than that of the ANN-11 model, and its value of the M5P model is 4302% more. In addition, the MAE values of ANN-5 and M5P models are 333% and 548% higher than that of the ANN-11 model, respectively. ANN-11 model has the best performance due to its R indicator value that is 0.99. This indicator value in the M5P and ANN-5 models is 0.95 and 0.94, respectively. According to SI indicator of ANN-11 model, it has an excellent performance with value of 0.03 while its value of ANN-5 and M5P models has a slight difference and cause a good performance. In addition, the M5P model has the highest value of OBJ, so it is 294% more than ANN-11. The ANN-5 model's OBJ value also is 217% higher than that of the ANN-11 model. It can be observed that the elastic modulus of concrete is overestimated by ANN-5 model due to MBE while this indicator shows that ANN-11 and M5P models underestimate the elastic modulus of concrete.

Table 6 The statistical indicators of ANN-11, ANN-5, and M5P tree models.

Models	RMSE (MPa)	MAE (MPa)	MAPE (%)	R	SI	MBE (MPa)	OBJ (MPa)
ANN-11	0.77	0.39	1.79	0.99	0.03	-0.02	1.05
ANN-5	2.72	1.69	8.33	0.94	0.11	0.12	3.33
M5P	3.39	2.53	13.36	0.95	0.14	-21	4.14

Predicted results against experimental results of the developed models for training and testing datasets is represented in Fig. 6. In fact, each sub-figure shows the linear regression model. It can be indicated from graphs that ANN-11 is more capable in learning and generalization phases since predicted results of ANN-11 are similar to experimental results more than that of other two models.

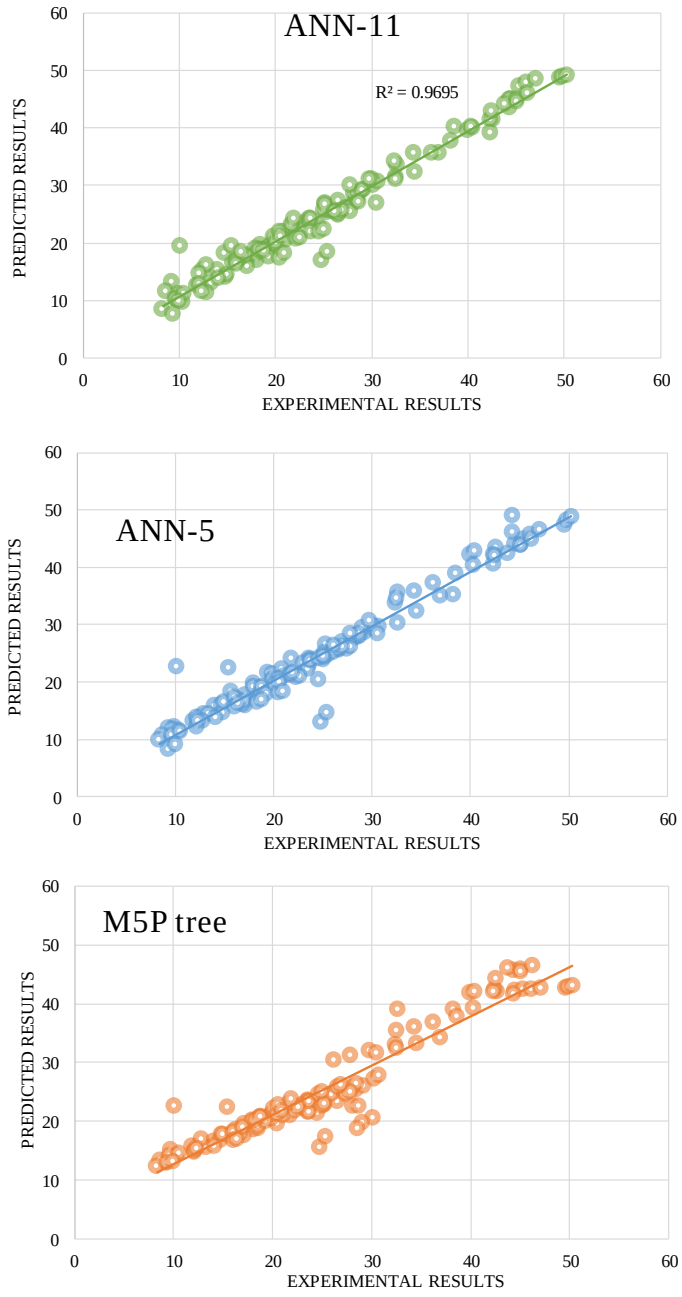

Figure 6 Predicted results vs experimental results of the developed models for training and testing datasets.

To compare the performance of different developed models, in terms of standard deviation, Correlation coefficient, and RMSE, Taylor diagram was used. The efficiency of models can be measured using a baseline that is in this diagram. The closer distance to the line, the more efficient model. A

Taylor diagram is demonstrated in Fig. 7 to compare the performance of the M5P and selected ANNs. As it can be seen, ANN-11 is the closest model to the baseline followed by ANN-5 while the farthest model is M5P tree.

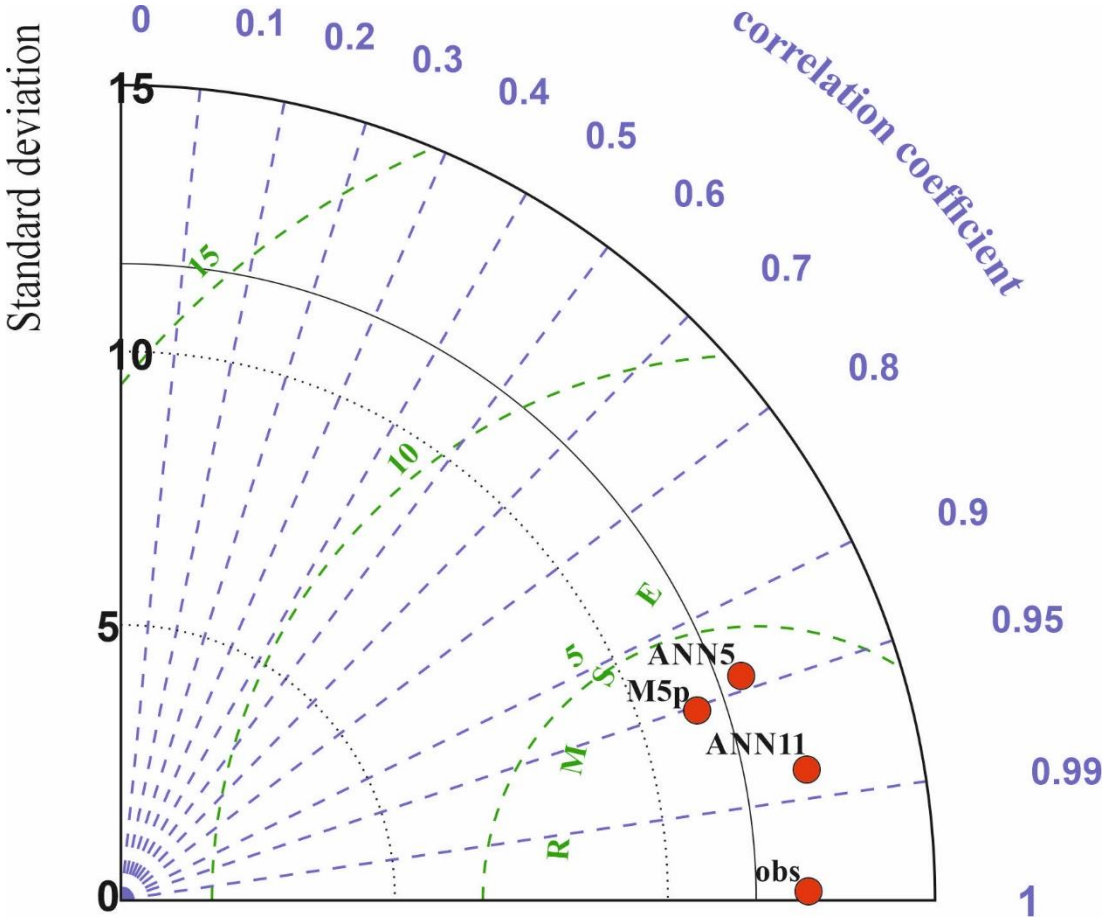

Figure 7 Taylor diagram of three developed models.

Using weights and biases of the selected models on the Appendix and the decision tree represented in the Fig. 5 civil engineers can estimate the elastic modulus of a concrete mixture containing GGBFS and optimized design of concrete is reachable by trial and error. Also, reducing environmental impact of concrete had been approached by many studies by utilizing the use of high quality recycled aggregate as well which can be recommended for the future studies [49-51].

Conclusions

To predict the elastic modulus of concrete containing GGBFS, an ANN model was developed, which can save in cost, time, and energy and accounts for both simplicity and accuracy. In this study, in the proposed model (MOANN) the architecture of ANN was optimized using MOSSA. The following findings were drawn in this study:

- The obtained Pareto front includes 12 ANN models with various structures and precisions, which let the user choose among the 12 models based on the required accuracy and simplicity.
- Pearson correlation coefficient of eight of 12 non-dominated ANN models on the Pareto front was more than 0.90, which shows the great correlation between the predicted and experimental results.
- Even the accuracy of the simple developed ANN model with just 17 links was acceptable with the root mean squared error of 2.72 MPa and the mean absolute percentage error of 8.33%.
- The ANN-12 model with 6-8-6-1 architecture and 117 links is the most complicated and accurate one and the ANN model without any hidden layer is the simplest and the least accurate one.
- Comparing the performance of the two chosen ANN models with the M5P model tree indicates that the performance of even ANN-5 is better than M5P tree performance almost in all areas, and ANN-11 has a much better performance in comparison with M5P.

References

[1] K.P. Verian, A. Behnood, Effects of deicers on the performance of concrete pavements containing air-cooled blast furnace slag and supplementary cementitious materials, Cem. Concr. Compos. 90 (2018) 27–41.

[2] J. Peng, L. Huang, Y. Zhao, P. Chen, L. Zeng, W. Zheng, Modeling of carbon dioxide measurement on cement plants, Adv. Mater. Res. 610–613 (2013) 2120–2128. doi:10.4028/www.scientific.net/AMR.610-613.2120.

[3] C. Li, X. Gong, S. Cui, Z. Wang, Y. Zheng, B. Chi, CO2 emissions due to cement manufacture, Mater. Sci. Forum. 685 (2011) 181–187. doi:10.4028/www.scientific.net/MSF.685.181.

[4] C. Chen, G. Habert, Y. Bouzidi, A. Jullien, Environmental Impact of Cement Production: Detail of The Different Processes and Cement Plant Variability Evaluation, J. Clean. Prod. 18 (2010) 478–485. doi:10.1016/j.jclepro.2009.12.014.

[5] C. Meyer, The greening of the concrete industry, Cem. Concr. Compos. 31 (2009) 601–605. doi:http://dx.doi.org/10.1016/j.cemconcomp.2008.12.010.

[6] C. Bilim, C.D. Atiş, H. Tanyildizi, O. Karahan, Predicting the compressive strength of ground granulated blast furnace slag concrete using artificial neural network, Adv. Eng. Softw. (2009). doi:10.1016/j.advengsoft.2008.05.005.

[7] I. Yüksel, T. Bilir, Ö. Özkan, Durability of concrete incorporating non-ground blast furnace slag and bottom ash as fine aggregate, Build. Environ. 42 (2007) 2651–2659. doi:10.1016/j.buildenv.2006.07.003.

[8] A.K. Saha, P.K. Sarker, Expansion due to alkali-silica reaction of ferronickel slag fine aggregate in OPC and blended cement mortars, Constr. Build. Mater. 123 (2016) 135–142. doi:10.1016/j.conbuildmat.2016.06.144.

[9] M.L. Berndt, Properties of sustainable concrete containing fly ash, slag and recycled concrete aggregate, Constr. Build. Mater. 23 (2009) 2606–2613. doi:10.1016/j.conbuildmat.2009.02.011.

[10] A. Kandiri, E. Mohammadi Golafshani, A. Behnood, Estimation of the compressive strength of concretes containing ground granulated blast furnace slag using hybridized multi-objective ANN and salp swarm algorithm, Constr. Build. Mater. (2020). doi:10.1016/j.conbuildmat.2020.118676.

[11] A. Behnood, E.M. Golafshani, Predicting the compressive strength of silica fume concrete using hybrid artificial neural network with multi-objective grey wolves, J. Clean. Prod. (2018). doi:10.1016/j.jclepro.2018.08.065.

[12] A. Behnood, E.M. Golafshani, Machine learning study of the mechanical properties of concretes containing waste foundry sand, Constr. Build. Mater. (2020). doi:10.1016/j.conbuildmat.2020.118152.

[13] A. Behnood, V. Behnood, M. Modiri Gharehveran, K.E. Alyamac, Prediction of the compressive strength of normal and high-performance concretes using M5P model tree algorithm, Constr. Build. Mater. 142 (2017). doi:10.1016/j.conbuildmat.2017.03.061.

[14] İ.B. Topçu, M. Sarıdemir, Prediction of compressive strength of concrete containing fly ash using artificial neural networks and fuzzy logic, Comput. Mater. Sci. (2008). doi:10.1016/j.commatsci.2007.04.009.

[15] U. Atici, Prediction of the strength of mineral admixture concrete using multivariable regression analysis and an artificial neural network, Expert Syst. Appl. (2011). doi:10.1016/j.eswa.2011.01.156.

[16] B.K.R. Prasad, H. Eskandari, B.V.V. Reddy, Prediction of compressive strength of SCC and HPC with high volume fly ash using ANN, Constr. Build. Mater. (2009). doi:10.1016/j.conbuildmat.2008.01.014.

[17] M. Sarıdemir, İ.B. Topçu, F. Özcan, M.H. Severcan, Prediction of long-term effects of GGBFS on compressive strength of concrete by artificial neural networks and fuzzy logic, Constr. Build. Mater. (2009). doi:10.1016/j.conbuildmat.2008.07.021.

[18] S. Chithra, S.R.R.S. Kumar, K. Chinnaraju, F. Alfin Ashmita, A comparative study on the compressive strength prediction models for High Performance Concrete containing nano silica and copper slag using regression analysis and Artificial Neural Networks, Constr. Build. Mater. (2016). doi:10.1016/j.conbuildmat.2016.03.214.

[19] A.T.A. Dantas, M. Batista Leite, K. De Jesus Nagahama, Prediction of compressive strength of concrete containing construction and demolition waste using artificial neural networks, Constr. Build. Mater. (2013). doi:10.1016/j.conbuildmat.2012.09.026.

[20] M. Pala, E. Özbay, A. Öztaş, M.I. Yuce, Appraisal of long-term effects of fly ash and silica fume on compressive strength of concrete by neural networks, Constr. Build. Mater. (2007). doi:10.1016/j.conbuildmat.2005.08.009.

[21] M. Uysal, H. Tanyildizi, Predicting the core compressive strength of self-compacting concrete (SCC) mixtures with mineral additives using artificial neural network, Constr. Build. Mater. (2011). doi:10.1016/j.conbuildmat.2010.11.108.

[22] E.M. Golafshani, G. Pazouki, Predicting the compressive strength of self-compacting concrete containing fly ash using a hybrid artificial intelligence method, Comput. Concr. (2018). doi:10.12989/cac.2018.22.4.419.

[23] F. Özcan, C.D. Atiş, O. Karahan, E. Uncuoğlu, H. Tanyildizi, Comparison of artificial neural network and fuzzy logic models for prediction of long-term compressive strength of silica fume concrete, Adv. Eng. Softw. (2009). doi:10.1016/j.advengsoft.2009.01.005.

[24] E.M. Golafshani, A. Behnood, Estimating the optimal mix design of silica fume concrete using biogeography-based programming, Cem. Concr. Compos. 96 (2019) 95–105.

[25] A.J. Tenza-Abril, Y. Villacampa, A.M. Solak, F. Baeza-Brotons, Prediction and sensitivity analysis of compressive strength in segregated lightweight concrete based on artificial neural network using ultrasonic pulse velocity, Constr. Build. Mater. (2018). doi:10.1016/j.conbuildmat.2018.09.096.

[26] M.M. Alshihri, A.M. Azmy, M.S. El-Bisy, Neural networks for predicting compressive strength of structural light weight concrete, Constr. Build. Mater. (2009). doi:10.1016/j.conbuildmat.2008.12.003.

[27] Ł. Sadowski, M. Piechówka-Mielnik, T. Widziszowski, A. Gardynik, S. Mackiewicz, Hybrid ultrasonic-neural prediction of the compressive strength of environmentally friendly concrete screeds with high volume of waste quartz mineral dust, J. Clean. Prod. (2019). doi:10.1016/j.jclepro.2018.12.059.

[28] H. Naderpour, A.H. Rafiean, P. Fakharian, Compressive strength prediction of environmentally friendly concrete using artificial neural networks, J. Build. Eng. (2018). doi:10.1016/j.jobe.2018.01.007.

[29] M.A. Getahun, S.M. Shitote, Z.C. Abiero Gariy, Artificial neural network based modelling approach for strength prediction of concrete incorporating agricultural and construction wastes, Constr. Build. Mater. (2018). doi:10.1016/j.conbuildmat.2018.09.097.

[30] J. Xu, X. Zhao, Y. Yu, T. Xie, G. Yang, J. Xue, Parametric sensitivity analysis and modelling of mechanical properties of normal- and high-strength recycled aggregate concrete using grey theory, multiple nonlinear regression and artificial neural networks, Constr. Build. Mater. (2019). doi:10.1016/j.conbuildmat.2019.03.234.

[31] A. Behnood, J. Olek, M.A. Glinicki, Predicting modulus elasticity of recycled aggregate concrete using M5′ model tree algorithm, Constr. Build. Mater. (2015). doi:10.1016/j.conbuildmat.2015.06.055.

[32] E.M. Golafshani, A. Behnood, Automatic regression methods for formulation of elastic modulus of recycled aggregate concrete, Appl. Soft Comput. J. 64 (2018). doi:10.1016/j.asoc.2017.12.030.

[33] E.M. Golafshani, A. Behnood, Application of soft computing methods for predicting the elastic modulus of recycled aggregate concrete, J. Clean. Prod. (2017). doi:10.1016/j.jclepro.2017.11.186.

[34] A. Behnood, K.P. Verian, M. Modiri Gharehveran, Evaluation of the splitting tensile strength in plain and steel fiber-reinforced concrete based on the compressive strength, Constr. Build. Mater. 98 (2015) 519–529. doi:10.1016/j.conbuildmat.2015.08.124.

[35] E.M. Golafshani, A. Ashour, Prediction of self-compacting concrete elastic modulus using two symbolic regression techniques, Autom. Constr. 64 (2016) 7–19. doi:http://dx.doi.org/10.1016/j.autcon.2015.12.026.

[36] A. Behnood, E.M. Golafshani, Machine learning study of the mechanical properties of concretes containing waste foundry sand, Constr. Build. Mater. 243 (2020) 118152. doi:https://doi.org/10.1016/j.conbuildmat.2020.118152.

[37] D. Shen, Y. Jiao, Y. Gao, S. Zhu, G. Jiang, Influence of ground granulated blast furnace slag on cracking potential of high performance concrete at early age, Constr. Build. Mater. 241 (2020) 117839.

[38] R. Siddique, D. Kaur, Properties of concrete containing ground granulated blast furnace slag (GGBFS) at elevated temperatures, J. Adv. Res. (2012). doi:10.1016/j.jare.2011.03.004.

[39] R.N. Swamy, A. Bouikni, Some engineering properties of slag concrete as influenced by mix proportioning and curing, ACI Mater. J. (1990). doi:10.14359/2148.

[40] S. Samad, A. Shah, M.C. Limbachiya, Strength development characteristics of concrete produced with blended cement using ground granulated blast furnace slag (GGBS) under various curing conditions, Sadhana - Acad. Proc. Eng. Sci. (2017). doi:10.1007/s12046-017-0667-z.

[41] A. Gholampour, T. Ozbakkaloglu, Performance of sustainable concretes containing very high volume Class-F fly ash and ground granulated blast furnace slag, J. Clean. Prod. (2017). doi:10.1016/j.jclepro.2017.06.087.

[42] M. Shariq, J. Prasad, H. Abbas, Effect of GGBFS on age dependent static modulus of elasticity of concrete, Constr. Build. Mater. (2013). doi:10.1016/j.conbuildmat.2012.12.035.

[43] V. Sivasundaram, V.M. Malhotra, Properties of concrete incorporating low quantity of cement and high volumes of ground granulated slag, ACI Mater. J. (1992). doi:10.14359/4027.

[44] D. Elwell, G. Fu, Compression testing of concrete: Cylinders VS. cubes, Newyork State Department of Transportation, 1995.

[45] S. Mirjalili, A.H. Gandomi, S.Z. Mirjalili, S. Saremi, H. Faris, S.M. Mirjalili, Salp Swarm Algorithm: A bio-inspired optimizer for engineering design problems, Adv. Eng. Softw. (2017). doi:10.1016/j.advengsoft.2017.07.002.

[46] J.R. Quinlan, LEARNING WITH CONTINUOUS CLASSES: Constructing Model Trees, 5th Aust. Jt. Conf. Artif. Intell. (1992). doi:10.1.1.34.885.

[47] Y. Wang, I.H. Witten, Induction of model trees for predicting continuous classes, Proc. 9th Eur. Conf. Mach. Learn. Poster Pap. (1997).

[48] M.F. Li, X.P. Tang, W. Wu, H. Bin Liu, General models for estimating daily global solar radiation for different solar radiation zones in mainland China, Energy Convers. Manag. (2013). doi:10.1016/j.enconman.2013.03.004.

[49] F. Sartipi, "Automatic sorting of recycled aggregate using image processing and object detection," Journal of Construction Materials, vol. 1, pp. 3-3, 2020, doi: https://doi.org/10.36756/JCM.v1.2.1 .

[50] F. Sartipi and M. Soomro, "Solutions for barriers against the wider use of recycled aggregate."

[51] A. Todhunter, M. Crowley, M. Gholamisheverini, and F. Sartipi, "Advanced technological implementation of construction and demolition waste recycling," Journal of Construction Materials, vol. 1, no. 1, 2019, doi: https://doi.org/10.36756/JCM.v1.1.3 .

Appendix

Weights and biases of the ANN5 model

$$\text{Input layer weigths matrix} = \begin{bmatrix} 11.5964 & -0.9782 & 6.9339 & -1.072 & 25.4101 & 0.0797 \\ 2.7547 & 10.0614 & 1.9641 & 2.5931 & 3.7090 & -4.2398 \end{bmatrix}$$

$$\text{Input layer bias vector} = [1.3148 \quad -7.6512]$$

$$\text{Output layer weights vector} = [0.6966 \quad -0.3410]$$

$$\text{Output layer bias} = [-0.3786]$$

Weights and biases of the ANN11 model

$$\text{Input layer weigths matrix} = \begin{bmatrix} -1.3111 & 2.4062 & -0.8953 & 0.8341 & -3.6961 & 4.1058 \\ 0.0471 & -2.0815 & 0.1184 & -0.9495 & 1.0568 & -3.8008 \\ -0.0467 & -3.5863 & 1.0542 & -1.7990 & -0.4921 & -0.2038 \\ -0.7335 & -3.0438 & -4.6157 & -0.6216 & 4.8839 & -0.1971 \\ -2.4741 & 0.3669 & -1.4637 & -1.3632 & 0.1869 & -0.0293 \end{bmatrix}$$

$$\text{Input layer bias vector} = [3.08053211201657 \quad -3.3807 \quad 1.3834 \quad 0.3417 \quad -2.1763]$$

$$\text{Hidden layer weights matrix} = \begin{bmatrix} -1.0811 & 0.6336 & -0.9583 & 5.4708 & 1.1786 \\ 0.9378 & 1.9049 & 2.3174 & -2.4114 & -0.3490 \\ -0.9738 & -1.2339 & 0.8933 & 0.4735 & -0.7636 \\ 1.0416 & 1.8000 & 0.6296 & 0.2780 & 0.7683 \\ 0.9383 & 1.2837 & -0.6819 & 1.16648 & 2.0636 \end{bmatrix}$$

$$\text{Hidden layer bias vector} = [1.1063 \quad 0.9172 \quad -0.3808 \quad 1.7325 \quad -0.8267]$$

$$\text{Output layer weights vector} = [0.9560 \quad 1.0102 \quad 1.8220 \quad -3.0072 \quad -0.7580]$$

$$\text{Output layer bias vector} = [-0.6707]$$